Published in final edited form as:
J Phys Chem Lett. ; 4(16): 2605–2609. doi:10.1021/jz401443q.

Unraveling the Primary Isomerization Dynamics in Cyanobacterial Phytochrome Cph1 with Multi-pulse Manipulations

Peter W. Kim[1], **Nathan C. Rockwell**[2], **Lucy H. Freer**[1], **Che-Wei Chang**[1], **Shelley S. Martin**[2], **J. Clark Lagarias**[2], and **Delmar S. Larsen**[1,*]

[1]Department of Chemistry, University of California, One Shields Avenue, Davis, CA 95616

[2]Department of Molecular and Cell Biology, University of California, One Shields Avenue, Davis, CA 95616

Abstract

The ultrafast mechanisms underlying the initial photoisomerization ($P_r \rightarrow$ Lumi-R) in the forward reaction of the cyanobacterial photoreceptor Cph1 were explored with multipulse pump-dump-probe transient spectroscopy. A recently postulated multi-population model was used to fit the transient pump-dump-probe and dump-induced depletion signals. We observed dump-induced depletion of the Lumi-R photoproduct, demonstrating that photoisomerization occurs via evolution on both the excited- and ground-state electronic surfaces. Excited-state equilibrium was not observed, as shown via the absence of a dump-induced excited-state "Le Châtelier redistribution" of excited-state populations. The importance of incorporating the inhomogeneous dynamics of Cph1 in interpreting measured transient data is discussed.

Keywords

photoreceptors; transient absorption; phytochromes; excited-state dynamic; pump-dump-probe

Cyanobacteria hold great potential for bioenergy production due to their ability to fix both carbon and nitrogen. Like other photosynthetic organisms, they exploit photosensory proteins to optimize light capture and energy conversion. Understanding how these photoreceptors operate facilitates the engineering of cyanobacteria as sustainable energy sources and enhances our understanding of light utilization by biological systems.[1] Cph1 is a red/far-red photochromic phytochrome from the cyanobacterium Synechocystis sp. PCC 6803.[2-3] Absorption of red light by the dark-adapted P_r state triggers rapid isomerization about the 15,16 double bond of the covalently bound phycocyanobilin (PCB, Figure 1A) chromophore, yielding the isomerized primary Lumi-R photoproduct intermediate.[4-6] Lumi-R subsequently evolves via transient Meta-R_a and Meta-R_c intermediates to form the metastable far-red-absorbing P_{fr} signaling state.[7-8] This reversible photoisomerization modulates the activity of a histidine kinase output domain and downstream signaling that is still unknown.[2]

The near-IR (NIR) fluorescence of Cph1, and phytochromes in general, is an attractive feature for fluorescent medical probe development because of NIR's deeper tissue

*Corresponding Author: dlarsen@ucdavis.edu.

Supporting Information **Available**: Experimental procedures and supplementary results are available free of charge via the Internet at http://pubs.acs.org.

penetrability. Recently, bacterial phytochromes have been engineered to increase its fluorescence quantum yield (ϕ_{fluor}) as an in vivo fluorescence probes.[9-11] Cph1 itself can be converted into a NIR fluorescent protein by a single Y176H mutation in the chromophore-binding pocket.[12] Phytochrome photoswitching has also led to the development of optogenetic systems based on Cph1 and related sensors.[11, 13] For fluorophore development, the photochemical quantum yield (ϕ_{photo}) and radiationless deexcitation processes must be suppressed to enhance fluorescence. The partition between fluorescence, photoconversion and non-radiative pathways is dictated by the excited-state dynamics of the photosensory protein. Thus, studying excited-state evolution of phytochromes is greatly beneficial to understanding protein-engineering principals underlying development of efficient fluorophore and/or optogenetic materials.

Recently, the low ϕ_{photo} of Cph1 (10-15%) was rationalized in terms of a novel photoisomerization model whereby isomerization occurs fully on the excited-state potential surface.[14] In this model, formation of electronically excited Lumi-R* occurs on a 3-ps time scale, after which internal conversion populates the ground-state Lumi-R intermediate with a 30-ps time constant (Figure 1B, τ_2 and τ_3, respectively). This 'excited-state isomerization' model is based on the observation that structurally sensitive vibrational modes characteristic of full isomerization appear on a 3-ps time scale, while stimulated emission (SE) signals from the electronically excited state persist beyond 30 ps. These data were interpreted as indicating that photoisomerization is completed on the excited-state potential energy surface; that is, that the relaxed pre-isomerized I* excited-state species forms the fully isomerized excited-state Lumi-R* population before conversion to the ground electronic state. This contrasts with the more established 'mixed-state' isomerization model developed for other photosensors. In a mixed-state model, the electronically excited population evolves on the excited-state potential energy surface until encountering an avoided or true crossing (Conical Intersection, CI) with the ground-state potential energy surface (Figure 1C).[15] This induces the rapid non-adiabatic repopulation of the ground state to complete the isomerization reaction with non-unity yield and without the accumulation of electronically excited photo-intermediates such as Lumi-R*.

An intriguing aspect of the proposed excited-state isomerization model (Figure 1B) is the implication that I* and Lumi-R* are in equilibrium. This equilibrium was a necessary in the excited-state isomerization model to reproduce the experimentally determined ϕ_{photo} of 15 % (Figure S1A).[3] Without this equilibrium, an unreasonably high ϕ_{photo} of 50 % is predicted (Figure S1B). A similar excited-state equilibrium has been invoked to interpret the multi-exponential decay kinetics observed in time-resolved fluorescence spectra of oat phytochrome.[16] Similar multi-exponential excited-state time constants were also observed with different spectroscopic techniques, including our current results (Figure S6A).[6, 17]

The excited-state isomerization model (Figure 1B) incorporates the assumption that Cph1's forward dynamics and ϕ_{photo} result from a homogeneous excited-state population, such that the photoproduct and SE signals arise from the same photoexcited population.[18] However, our recent temperature and excitation-dependent study of Cph1 revealed heterogeneous populations[19]: a productive population with faster excited-state dynamics and a fluorescent population with slow excited-state dynamics similar to the Y176H variant.[12] Ground-state heterogeneity of the Cph1 P_r state was also recently observed by solid-state NMR.[20]

Several other phenomena imply a heterogeneous P_r state: a blue-shifted fluorescent excitation spectrum compared to the absorbance spectrum,[21] temperature-dependent absorption spectra with a clear isosbestic point at ambient temperature level,[18] and excitation-dependent kinetics.[6] A new heterogeneous model of the Cph1 forward reaction[19] rationalizes these data corroborating the observed low ϕ_{photo} without the need for an

excited-state equilibrium. In light of the observed heterogeneity, a key assumption of the excited-state isomerization model is not valid, so it becomes necessary to re-examine the excited-state mechanisms. We have focused on signals in the visible region of the spectrum because the heterogeneous model was constructed to describe such signals.

Although a powerful technique, visible transient absorption or pump-probe (PP) spectroscopy has limitations for exploring the underlying dynamics of Cph1 due to the significant overlap of the SE from the excited-state, the ground-state absorptions of P_r, and the Lumi-R photoproduct (Figure 2B). To identify which model accurately describes the primary excited-state isomerization dynamics of Cph1, we therefore applied the more powerful multi-pulse ultrafast pump-dump-broadband probe (PDP) spectroscopy.[22-25] PDP techniques have been used to resolve underlying dynamics and populations that were not easily extracted from PP signals alone such as ground-state dynamics.[23-26]

Here, we use the PDP technique to verify which isomerization model is applicable for Cph1 by resolving the dump-induced effects on the change in Lumi-R photoproduct yield. In the case of excited-state isomerization, de-excitation of Lumi-R* photoproduct by the dump pulse would increase Lumi-R yield since some remaining I* following the dump pulse also could convert to Lumi-R* (Figure 3A). By contrast, in the mixed-state model with isomerization proceeding through a conical intersection, Lumi-R would form on the ground-state surface at the same timescale as the excited-state decay (30 ps), so a more rapid dump pulse would deplete the excited state and reduce Lumi-R yield (Figure 3B). We used a 725 nm dump pulse with a narrow spectral band ($\Delta\lambda_{FWHM}$ = 7 nm) at 10 ps or 2.3 ps after excitation (615 nm pump pulse: Figure 2A). 725 nm overlaps the SE band both spectrally and temporally at ≤ 10 ps (Figure 2B, red curve) but does not overlap the ground-state absorption spectra of P_r or Lumi-R (Figure 2A black and 2B magenta curves, respectively). Although a hidden ESA band overlapping with SE may initiate $S_1 \rightarrow S_n$ re-pumping to interfere with PDP signals,[27-28] the NIR PP dynamics suggests it is a negligible (<10 %) contribution to the dump-induced dynamics (Figure S3). Hence the PDP signals can be interpreted exclusively as dump-induced dynamics.[27-28]

The 725-nm dump pulse is also resonant with the P_{fr} state.[29] To reduce the dump-initiated back reaction, $P_{fr} \rightarrow P_r$, the flowing sample was continually back-illuminated with a 720-nm LED light source (Epitex inc., L720-66-60). A small amplitude (noise level after 1 ps) of back reaction was initiated with near identical dynamics to those previously reported (Figure S2).[29] However, since this signal is independent from the forward dynamics (i.e., different originating populations), simply subtracting this dump-probe (DP) signal from the PDP signals removes its effect and does not adversely affect the data analysis or interpretation.

Within the fully excited-state isomerization model (Figure 2B), the I* state forms rapidly and then decays to P_r and equilibrates with Lumi-R*. The 10-ps dump pulse would de-excite I* to repopulate the P_r state, but Lumi-R* would de-excite to generate Lumi-R instead (Figure S1A). In the absence of an excited-state equilibration between I* and Lumi-R*, the dump would have zero effect on the terminal Lumi-R population, as isomerization would be completed prior to dumping (Figure S1B). Should an excited-state equilibrium exist, the dump-induced depletion of Lumi-R* would be partially refilled by I* (an “excited-state Le Châtelier’s Principle” in action), increasing the terminal Lumi-R population (Figure 3A, magenta curves). However, if isomerization were incomplete at 10 ps (the mixed-state model, Figure 1C and S1C), the dump pulse would repopulate the ground-state P_r population, resulting in decreased Lumi-R formation (Figure 3B). Resolving reduced Lumi-R formation after a dump pulse at 10 ps would thus demonstrate that the electronically excited photoproduct Lumi-R* does not accumulate.

Figures 4A and B show experimental PP (red circles) and PDP - DP (blue triangles) signals at 500 nm (ESA) and 695 nm (overlapping SE and Lumi-R). The PDP – DP signal exhibits a sharp depletion of the excited state immediately after the 10-ps dump pulse (see insets). This depletion is observed spectrally in the 11-ps spectra measured 1 ps after the dump pulse (Figure 5A), with clear reduction of both negative SE and positive ESA bands. Furthermore, the bleach band peaking at ~665 nm is also depleted, because the dumped population refills in the P_r population.

The dumped population has undergone evolution on the excited-state surface, so the dump pulse typically generates a twisted (or vibrationally excited) ground-state intermediate (GSI) population that can be resolved in the deviation of the ΔΔOD from the inverted PP spectrum.[26, 30] Therefore, the PP and ΔΔOD signals immediately after dumping can be compared to extract dump-induced GSI kinetics (spectra and timescales). Such analysis extracted GSI population in the phytochrome-related cyanobacteriochrome NpR6012g4, which also demonstrated to form Lumi-R on the ground-state surface.[26] Other PDP studies on Cph1 forward dynamics suggested the presence of a GSI,[27-28] however, the PDP signals in this study (i.e., comparison between PP and ΔΔOD from 10-ps and 2.3-ps PDP signals) exhibited no clear evidence for meta-stable GSI populations (Figures S8-S11).

To resolve the dump-induced effects on Lumi-R yield, the Lumi-R population must be cleanly resolved free from overlapping ESA, SE, or GSI transitions. The weak amplitude of the Lumi-R absorption signal (1.4 mOD at 695 nm) is easily contaminated by overlapping SE signals (Figure 2B). Therefore, the Lumi-R population was analyzed at 5 ns, when >99 % of the excited-state population is depleted (Figure S7A). The Lumi-R spectrum (Figure 5B, black curve) exhibited a positive band from 680-710 nm and bleach from 625-680 nm. The ΔΔOD curve clearly indicates a dump-induced depletion of Lumi-R that regenerate the original P_r population.

The observation of dump-induced Lumi-R depletion at 10 ps (Figure 5B) validates the mixed-state model and refutes the excited-state isomerization model for Cph1. Similar results were obtained with the faster dump pulse at 2.3 ps (Figures S5, S10, S11, and S14-S17). We employed our previous inhomogeneous model developed from temperature and excitation-dependent PP experiments,[19] allowing global analysis of the complete 10-ps and 2.3-ps dumped PDP datasets. This analysis is shown in Figures S12 (10 ps) and S14 (2.3 ps), with excellent agreement to the data (Figure 4 and S13 for 10-ps dump, and Figure S15 for 2.3-ps dump). Moreover, this new model extracts consistent spectra of heterogeneous subpopulations between independently measured PDP signals here and in the temperature-dependent study (Figure S16).

Our results above conflict with recent PDP experiments on Cph1 using mid-IR and VIS probing.[27-28] This work used dump pulses at 1 and 14 ps after excitation, with an apparent dump-induced increase of Lumi-R yield. However, the analysis was considerably complicated by significant (re)pumping dynamics of the P_r ground state, Lumi-R, and ESA bands, resulting from a broad dump pulse (620 to 680 nm) overlapping all three bands (Figures 2 and 5). The broad dump pulse obscures dump-induced effects, and characterization of the true depletion of the terminal Lumi-R population is difficult unless the complete underlying inhomogeneous dynamics (including the spectral and temporal properties of each sub-population) are accounted for. We avoided such complications through use of a narrow dump pulse centered at 725-nm, through analysis of the late 5-ns signals, and through use of the heterogeneous model allowing global analysis of multiple independent datasets.

To conclude, the broadband PDP signals and analysis presented above provide no evidence for the accumulation of the Lumi-R* intermediate or for an excited-state equilibrium within Cph1, inferred previously from analysis of FSRS experimental data.[14] Our observations support an isomerization proceeding via partial evolution on the excited-state surface with completion upon quenching to the ground state (presumably via a canonical intersection after an excited-state barrier: Figure 6) and relaxation on the ground-state surface to generate Lumi-R. In such a view, the transient dynamics of Cph1 (including FSRS signals) can best interpret by the coexisting evolution of multiple sub-populations, with fast Lumi-R formation from a productive sub-population that coexists with slower-decaying sub-populations having higher fluorescence.

Experiment

Protein was purified after recombinant expression in *E. coli* cells engineered to produce phycocyanobilin (PCB) exactly as described.[31] The PDP experiment was conducted as previously described[26] and more detailed information can be found in Supporting Information. The primary ultrafast laser source was an amplified Ti:sapphire laser system (Spectra Physics Spitfire Pro) that delivered 800-nm pulses with a 2.3-mJ pulse energy at a 1-kHz repetition rate and 40-fs full width at half maximum (FWHM) pulse duration. The laser output was split into three separate pathways for generating pump, dump and probe pulses. The broadband white light probe pulses were generated, which was then focused onto the sample and dispersed by commercial spectrograph (Oriel MS125) to be detected with a linear 256-pixel photodiode array (Hamamatsu S3901 and C7884). The pump and dump pulses were generated by home-built non-collinear optical parametric amplifiers (NOPA).[32] The pump pulses had a 615-nm central wavelength with 30-nm FWHM bandwidth and 300-nJ pulse energy. The dump pulse had a 725 nm with 10-nm FWHM bandwidth with 900-nJ pulse energy. The instrumental response functions for pump and dump pulses were 100 fs and 150 fs, respectively. The probe beam was optically delayed with respect to the pump pulse with a computer controlled linear-motor stage (Newport IMS600LM), which allowed up to 7-ns temporal separation. The dump beam was also delayed 2.3 and 10 ps after the pumping to generate two independent PDP datasets (collected on different days). The pump and dump pulses were linearly polarized (parallel) to each other and set to 54.7° (magic angle) with respect to probe pulse polarization. The sample was flowed continuously in a closed circuit to ensure fresh sample for each excitation pulse. The path length of the quartz cuvette was 2 mm, and the optical density at the red absorbance band was 0.4-0.5 at that path length. All experiments were performed at room temperature.

Supplementary Material

Refer to Web version on PubMed Central for supplementary material.

Acknowledgments

This work was supported by grants from the Chemical Sciences, Geosciences, and Biosciences Division, Office of Basic Energy Sciences, Office of Science, United States Department of Energy (DOE DE-FG02-09ER16117) to both J.C.L. and D.S.L. and the National Institutes of Health (GM068552) to J.C.L.

REFERENCES

(1). Kehoe DM, Gutu A. Responding to color: The Regulation of Complementary Chromatic Adaptation. Annu. Rev. Plant Biol. 2006; 57:127–150. [PubMed: 16669758]

(2). Yeh KC, Wu SH, Murphy JT, Lagarias JC. A Cyanobacterial Phytochrome Two-component Light Sensory System. Science. 1997; 277:1505–1508. [PubMed: 9278513]

(3). Lamparter T, Mittmann F, Gartner W, Borner T, Hartmann E, Hughes J. Characterization of Recombinant Phytochrome from the Cyanobacterium Synechocystis. Proc. Natl. Acad. Sci. 1997; 94:11792–11797. [PubMed: 9342316]

(4). Rockwell NC, Su YS, Lagarias JC. Phytochrome Structure and Signaling Mechanisms. Annu. Rev. Plant Biol. 2006; 57:837–858. [PubMed: 16669784]

(5). Essen LO, Mailliet J, Hughes J. The Structure of a Complete Phytochrome Sensory Module in the Pr Ground State. Proc. Natl. Acad. Sci. 2008; 105:14709–14714. [PubMed: 18799745]

(6). Heyne K, Herbst J, Stehlik D, Esteban B, Lamparter T, Hughes J, Diller R. Ultrafast Dynamics of Phytochrome from the Cyanobacterium Synechocystis, Reconstituted with Phycocyanobilin and Phycoerythrobilin. Biophys. J. 2002; 82:1004–1016. [PubMed: 11806940]

(7). Kneip C, Hildebrandt P, Schlamann W, Braslavsky SE, Mark F, Schaffner K. Protonation State and Structural Changes of the Tetrapyrrole Chromophore During the Pr → Pfr Phototransformation of Phytochrome: A Sesonance Raman Spectroscopic Study. Biochemistry. 1999; 38:15185–15192. [PubMed: 10563801]

(8). van Thor JJ, Borucki B, Crielaard W, Otto H, Lamparter T, Hughes J, Hellingwerf KJ, Heyn MP. Light-induced Proton Release and Proton Uptake Reactions in the Cyanobacterial Phytochrome Cph1. Biochemistry. 2001; 40:11460–11471. [PubMed: 11560494]

(9). Shu XK, Royant A, Lin MZ, Aguilera TA, Lev-Ram V, Steinbach PA, Tsien RY. Mammalian Expression of Infrared Fluorescent Proteins Engineered from a Bacterial Phytochrome. Science. 2009; 324:804–807. [PubMed: 19423828]

(10). Auldridge ME, Satyshur KA, Anstrom DM, Forest KT. Structure-guided Engineering Enhances a Phytochrome-based Infrared Fluorescent Protein. J. Biol. Chem. 2012; 287:7000–7009. [PubMed: 22210774]

(11). Piatkevich KD, Subach FV, Verkhusha VV. Engineering of Bacterial Phytochromes for Near-infrared Imaging, Sensing, and Light-control in Mammals. Chem. Soc. Rev. 2013; 42:3441–3452. [PubMed: 23361376]

(12). Fischer AJ, Lagarias JC. Harnessing Phytochrome's Glowing Potential. Proc. Natl. Acad. Sci. 2004; 101:17334–17339. [PubMed: 15548612]

(13). Tabor JJ, Levskaya A, Voigt CA. Multichromatic Control of Gene Expression in Escherichia coli. J. Mol. Biol. 2011; 405:315–324. [PubMed: 21035461]

(14). Dasgupta J, Frontiera RR, Taylor KC, Lagarias JC, Mathies RA. Ultrafast Excited-state Isomerization in Phytochrome Revealed by Femtosecond Stimulated Raman Spectroscopy. Proc. Natl. Acad. Sci. 2009; 106:1784–1789. [PubMed: 19179399]

(15). Schapiro I, Melaccio F, Laricheva EN, Olivucci M. Using the Computer to Understand the Chemistry of Conical Intersections. Photochem. Photobiol. Sci. 2011; 10:867–886. [PubMed: 21373700]

(16). Holzwarth AR, Venuti E, Braslavsky SE, Schaffner K. The Phototransformation Process in Phytochrome. Ultrafast Fluorescence Component and Kinetic Models for the Initial Pr → Pfr Transformation Steps in Native Phytochrome. Biochim. Biophys. Acta. 1992; 1140:59–68.

(17). van Thor JJ, Ronayne KL, Towrie M. Formation of the Early Photoproduct Lumi-R of Cyanobacterial Phytochrome Cph1 Observed by Ultrafast Mid-infrared Spectroscopy. J. Am Chem. Soc. 2007; 129:126–132. [PubMed: 17199291]

(18). Spillane KM, Dasgupta J, Lagarias JC, Mathies RA. Homogeneity of Phytochrome Cph1 Vibronic Absorption Revealed by Resonance Raman Intensity Analysis. J. Am Chem. Soc. 2009; 131:13946–13948. [PubMed: 19739629]

(19). Kim, PW.; Rockwell, NC.; Martin, SS.; Lagarias, J.; Clark; Larsen, DS. Dynamic Inhomogeneity in the Cyanobacterial Phytochrome Cph1. 2013. In preparation

(20). Song C, Psakis G, Lang C, Mailliet J, Gartner W, Hughes J, Matysik J. Two Ground State Isoforms and a Chromophore D-ring Photoflip Triggering Extensive Intramolecular Changes in a Canonical Phytochrome. Proc. Natl. Acad. Sci. 2011; 108:3842–3847. [PubMed: 21325055]

(21). Mailliet J, Psakis G, Feilke K, Sineshchekov V, Essen L-O, Hughes J. Spectroscopy and a High-Resolution Crystal Structure of Tyr263 Mutants of Cyanobacterial Phytochrome Cph1. J. Mol. Biol. 2011; 413:115–127. [PubMed: 21888915]

(22). Gai F, McDonald JC, Anfinrud PA. Pump-dump-probe Spectroscopy of Bacteriorhodosin: Evidence for a Near-IR Excited State Absorbance. J. Am Chem. Soc. 1997; 119:6201–6202.

(23). Larsen DS, Vengris M, van Stokkum IHM, van der Horst MA, Cordfunke RA, Hellingwerf KJ, van Grondelle R. Initial Photo-induced Dynamics of the Photoactive Yellow Protein Chromophore in Solution. Chem. Phys. Lett. 2003; 369:563–569.

(24). Kennis JTM, Larsen DS, Ohta K, Facciotti MT, Glaeser RM, Fleming GR. Ultrafast Protein Dynamics of Bacteriorhodopsin Probed by Photon Echo and Transient Absorption Spectroscopy. J. Phys. Chem. B. 2002; 106:6067–6080.

(25). Larsen DS, Papagiannakis E, van Stokkum IHM, Vengris M, Kennis JTM, van Grondelle R. Excited State Dynamics of Beta-carotene Explored with Dispersed Multi-pulse Transient Absorption. Chem. Phys. Lett. 2003; 381:733–742.

(26). Kim PW, Freer LH, Rockwell NC, Martin SS, Lagarias JC, Larsen DS. Second-Chance Forward Isomerization Dynamics of the Red/Green Cyanobacteriochrome NpR6012g4 from Nostoc punctiforme. J Am. Chem. Soc. 2012; 134:130–133. [PubMed: 22107125]

(27). van Wilderen L, Clark IP, Towrie M, van Thor JJ. Mid-Infrared Picosecond Pump-Dump-Probe and Pump-Repump-Probe Experiments to Resolve a Ground-State Intermediate in Cyanobacterial Phytochrome Cph1. J. Phys. Chem. B. 2009; 113:16354–16364. [PubMed: 19950906]

(28). Fitzpatrick AE, Lincoln CN, van Wilderen LJ, van Thor JJ. Pump-Dump-Probe and Pump-Repump-Probe Ultrafast Spectroscopy Resolves Cross Section of an Early Ground State Intermediate and Stimulated Emission in the Photoreactions of the Pr Ground State of the Cyanobacterial Phytochrome Cph1. J. Phys. Chem. B. 2012; 116:1077–88. [PubMed: 22098118]

(29). Kim PW, Pan J, Rockwell NC, Chang C-W, Taylor KC, Lagarias JC, Larsen DS. Ultrafast E to Z Photoisomerization Dynamics of the Cph1 Phytochrome. Chem. Phys. Lett. 2012; 549:86–92. [PubMed: 23554514]

(30). Larsen DS, Vengris M, van Stokkum IHM, van der Horst MA, de Weerd FL, Hellingwerf KJ, van Grondelle R. Photoisomerization and Photoionization of the Photoactive Yellow Protein Chromophore in Solution. Biophys. J. 2004; 86:2538–2550. [PubMed: 15041690]

(31). Rockwell NC, Shang L, Martin SS, Lagarias JC. Distinct Classes of Red/Far-red Photochemistry within the Phytochrome Superfamily. Proc. Natl. Acad. Sci. 2009; 106:6123–6127. [PubMed: 19339496]

(32). Cerullo G, Nisoli M, Stagira S, De Silvestri S. Sub-8-fs Pulses from an Ultrabroadband Optical Parametric Amplifier in the Visible. Opt. Lett. 1998; 23:1283–1285. [PubMed: 18087499]

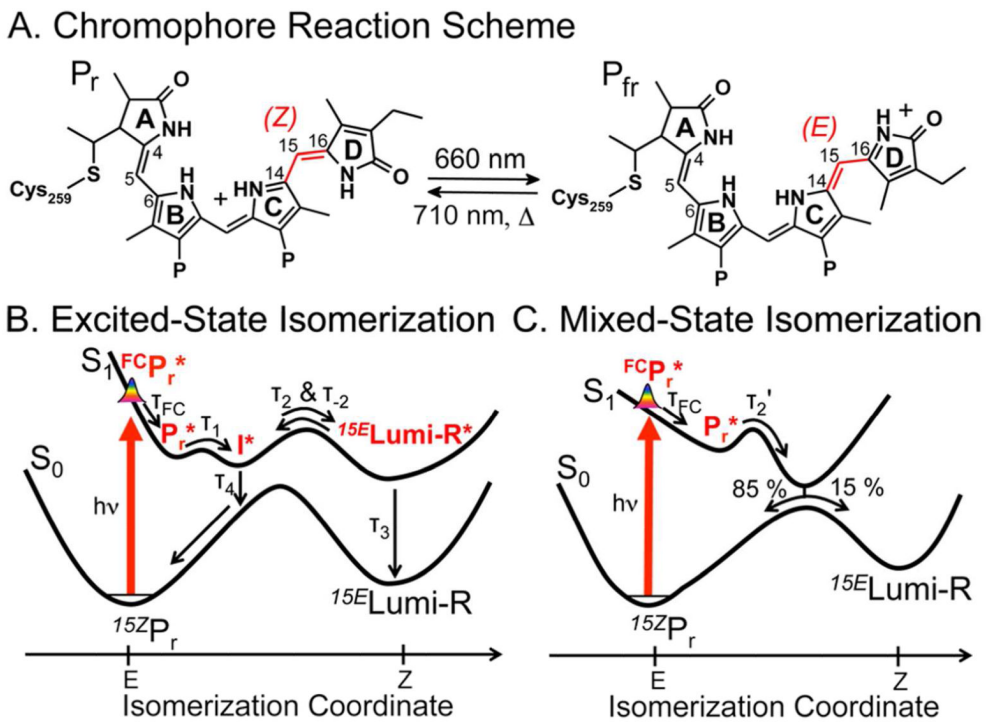

Figure 1.

Proposed mechanisms for Cph1 photoisomerization. (A) The phycocyanobilin (PCB) chromophore of Cph1 is shown with its Z to E photoreaction highlighted. P, propionate. (B) Full excited-state isomerization scheme proposed by Dasgupta et al. and (C) mixed-excited/ground state mechanism.

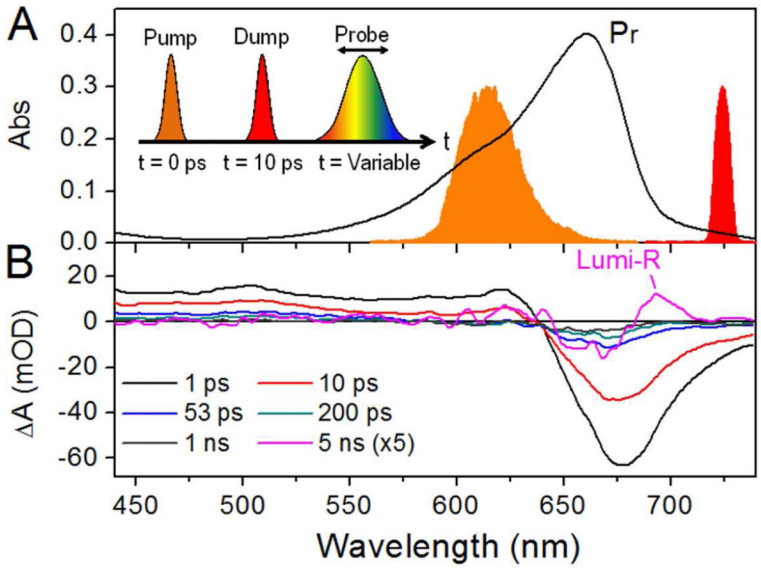

Figure 2.

Static and transient spectra of Cph1. (A) P_r absorption spectrum overlaid with pump (orange) and dump (red) pulses. Inset indicates the pump-dump-probe pulse sequence. (B) Pump-probe transient absorption spectra at select probe times. The 5-ns spectrum representing Lumi-R is magnified 5-fold for clarity.

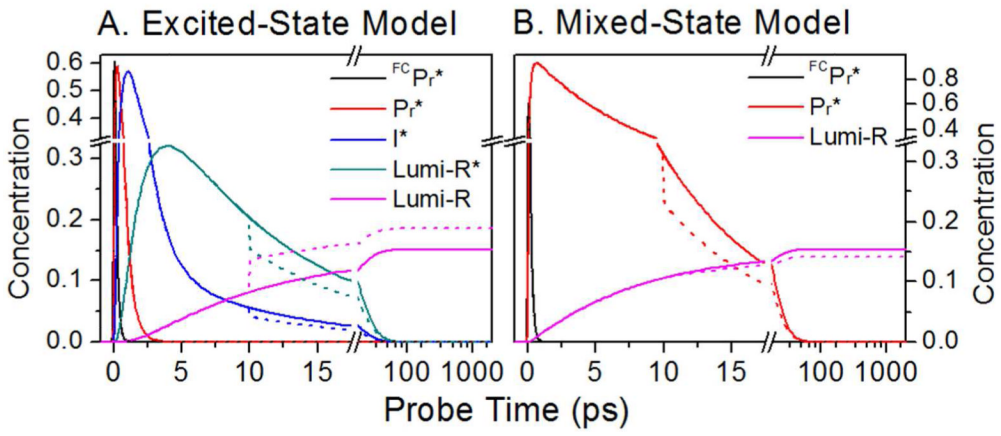

Figure 3.

Simulated effects of a dump pulse at 10 ps, leading to 30% depletion of the excited-state, for the excited-state isomerization (A) and mixed-state isomerization (B) models. The time constants used on the models from Figures 1B and 1C are: τ_{FC} = 150 fs, τ_1 = 500 fs, τ_2 = 3 ps, τ_{-2} = 6.5 ps, τ_2' = 55 ps, τ_3 = 30 ps, and τ_4 = 3 ps. The mixed model has non-unity Lumi-R yield at CI to make $\phi_{Lumi\text{-}R}$ = 15 %. Lines are simulated pump-probe (solid) and PDP (dashed) concentrations.

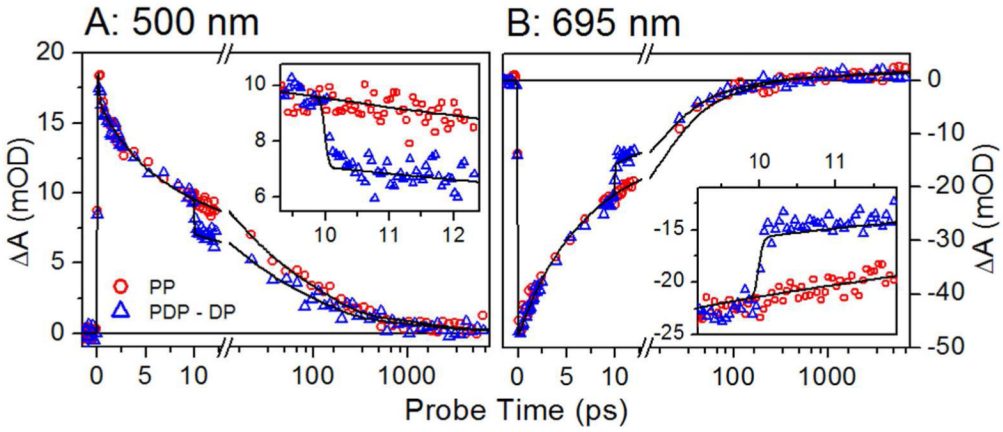

Figure 4.

Kinetic traces derived from transient PP (red) and PDP (blue) spectra are shown for representative probe wavelengths. (A) The ESA band at 500 nm; (B) SE and Lumi-R absorption at 695 nm. Insets show detail immediately after the dump pulse. The fits to the data (black curves) are simulated from the expanded model in Figure S12A.

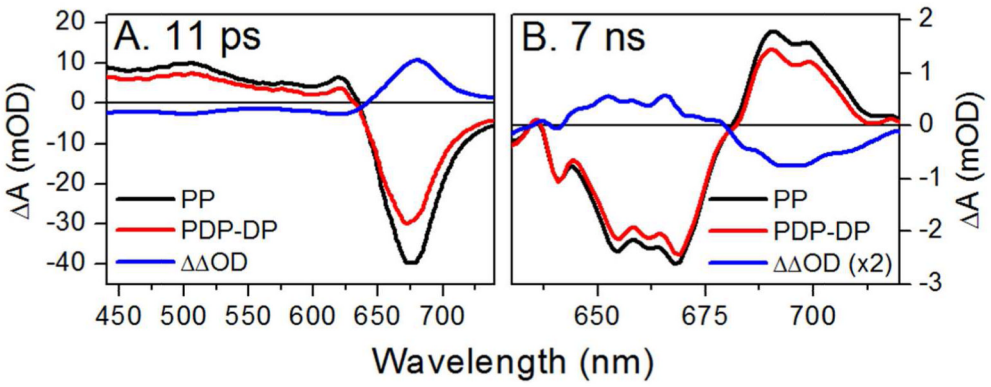

Figure 5.

Transient absorption difference spectra taken after 615-nm pump and 725-nm dump pulse at 10 ps. (A) the 11-ps spectra show initial depletion of the excited-state population and (B) the 7-ns spectra show terminal Lumi-R depletion.

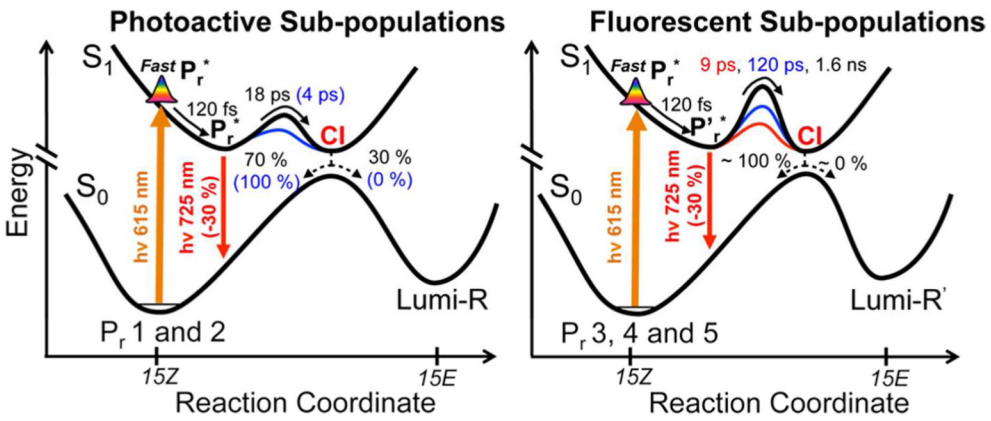

Figure 6.

Potential energy diagram describing the complete inhomogeneous photoisomerization model for P_r involving both photoactive and fluorescent populations.